

Determination of the pion distribution amplitude

Tao Huang,^{1,*} Tao Zhong,^{1,†} and Xing-Gang Wu^{2,‡}

¹*Institute of High Energy Physics and Theoretical Physics Center for Science Facilities,
Chinese Academy of Sciences, Beijing 100049, People's Republic of China*

²*Department of Physics, Chongqing University, Chongqing 401331, People's Republic of China*
(Received 5 June 2013; published 8 August 2013)

Currently, not enough is known to determine the hadron distribution amplitudes (DAs)—which are universal physical quantities in the high-energy processes involving hadrons—in order to apply perturbative QCD to exclusive processes. Even for the simplest pion, one cannot discriminate between different DA models. Conversely, one expects that processes involving pions can in principle provide strong constraints on the pion DA. For example, the pion-photon transition form factor (TFF) can get accurate information about the pion wave function or DA due to the single pion in this process. However, the data from Belle and *BABAR* show a big difference regarding this TFF in high- Q^2 regions; at present, they are unable to determine the pion DA. In the present paper, we think it is still possible to determine the pion DA as long as we perform a combined analysis of the existing data of the processes involving pions, such as $\pi \rightarrow \mu \bar{\nu}$, $\pi^0 \rightarrow \gamma \gamma$, $B \rightarrow \pi l \nu$, $D \rightarrow \pi l \nu$, etc. Based on the revised light-cone harmonic oscillator model, a convenient DA model is suggested, whose parameter B —which dominates its longitudinal behavior for $\phi_\pi(x, \mu^2)$ —can be determined in a definite range by these processes. A light-cone sum rule analysis of the semileptonic processes $B \rightarrow \pi l \nu$ and $D \rightarrow \pi l \nu$ leads to a narrow region $B = [0.01, 0.14]$, which indicates a slight deviation from the asymptotic DA. Then, one can predict the behavior of the pion-photon TFF in high- Q^2 regions which can be tested in future experiments. This method provides the possibility that the pion DA will be finally determined by a global fit.

DOI: [10.1103/PhysRevD.88.034013](https://doi.org/10.1103/PhysRevD.88.034013)

PACS numbers: 12.38.–t, 12.38.Bx, 14.40.Be

I. INTRODUCTION

In perturbative QCD (pQCD) theory, the distribution amplitude (DA) provides the underlying links between the hadronic phenomena in QCD at large distances (nonperturbative) and small distances (perturbative). The pion DA is an important element for applying pQCD calculations to the exclusive processes in the high-energy processes involving pions, and conversely these processes can in principle provide strong constraints on the pion DA. The pion DA is usually arranged according to its different twist structures. There are processes in which the contributions from the higher twists are highly power suppressed at short distances. For example, it has been found that the contribution to the pion-photon transition form factor (TFF) from higher-helicity and higher-twist structures is negligible [1,2]. Thus, these processes will provide good platforms to learn the properties of the leading-twist pion DA. It is well known that the leading-twist DA has the definite asymptotic form $\phi_\pi^{\text{as}}(x, \mu^2)|_{\mu^2 \rightarrow \infty} = 6x(1-x)$, which is independent of its shape around some initial scale $\mu_0 \sim \mathcal{O}(1 \text{ GeV})$. However, in practical calculations, it is important to know the correct shape of the pion DA at low and moderate scales.

The pion leading-twist DA at any scale μ can be expanded in Gegenbauer series in the following form [3,4]:

$$\phi_\pi(x, \mu^2) = 6x(1-x) \sum_{n=0}^{\infty} a_n(\mu^2) C_n^{3/2}(2x-1), \quad (1)$$

where $C_n^{3/2}(2x-1)$ are Gegenbauer polynomials and the nonperturbative coefficients $a_n(\mu^2)$ are Gegenbauer moments. Due to the isospin symmetry, only the even moments are nonzero. Usually the Gegenbauer series is convergent, and one can adopt the first several terms to analyze the experimental data. If the shape of the pion DA at an initial scale μ_0 is known, then one is assured of the following.

- (i) By using the orthogonality relations for the Gegenbauer polynomials, the Gegenbauer moments $a_n(\mu_0^2)$ can be obtained via the equation

$$a_n(\mu_0^2) = \frac{\int_0^1 dx \phi_\pi(x, \mu_0^2) C_n^{3/2}(2x-1)}{\int_0^1 dx 6x(1-x) [C_n^{3/2}(2x-1)]^2}. \quad (2)$$

- (ii) By using the QCD evolution equation [5], one can derive the pion DA at any other scale from $\phi_\pi(x, \mu_0^2)$.

The value of the Gegenbauer moments have been studied by using the nonperturbative approaches, such as QCD sum rules [6,7] or lattice QCD [8]. However, at present, there is no definite conclusion on whether the pion DA $\phi_\pi(x, \mu_0^2)$ is of the asymptotic form [5] or the CZ form [9], or even flat-like [10]. It would be helpful to have a general pion DA model that can mimic all the DA

*huangtao@ihep.ac.cn

†zhongtao@ihep.ac.cn

‡wuxg@cqu.edu.cn

behaviors suggested in the literature. For this purpose, one can first construct a wave-function (WF) model, since the pion DA is related to its WF $\Psi_\pi(x, \mathbf{k}_\perp)$ via the following relation:

$$\phi_\pi(x, \mu_0^2) = \frac{2\sqrt{6}}{f_\pi} \int_{|\mathbf{k}_\perp|^2 \leq \mu_0^2} \frac{d^2\mathbf{k}_\perp}{16\pi^3} \Psi_\pi(x, \mathbf{k}_\perp), \quad (3)$$

where f_π is the pion decay constant. It has been noted that a proper way of constructing the pion WF/DA is also very important for deriving a better end-point behavior in the small- x and small- k_\perp region for dealing with high-energy processes within the k_T -factorization approach [11], and thus for providing a better estimation for the pion-photon TFF, the pion electromagnetic form factor, etc.

The revised light-cone harmonic oscillator model for the pion leading-twist WF, and hence the model for the leading-twist DA, has been suggested in Refs. [12–14]. It has been found that by a proper change of the pion DA parameters, one can conveniently simulate the shape of the DA from the asymptotic-like to the CZ-like form. By comparing the theoretical estimations of the pionic processes with the corresponding experimental data, the undetermined parameters of the DA model can be fixed or at least greatly restricted. This is the purpose of the present paper.

More explicitly, we shall make a combined analysis of the pion DA by using the pion decay channels $\pi^0 \rightarrow \gamma\gamma$ and $\pi \rightarrow \mu\bar{\nu}$, the pion-photon TFF $F_{\pi\gamma}(Q^2)$, the semi-leptonic decays $B \rightarrow \pi l\nu$ and $D \rightarrow \pi l\nu$, and the exclusive process $B^0 \rightarrow \pi^0\pi^0$. For example, the pion-photon TFF $F_{\pi\gamma}(Q^2)$ that relates the pion with two photons provides the simplest example of the perturbative application to exclusive processes. In the lower-energy region the data on the pion-photon TFF measured by CELLO, CLEO, BABAR, and Belle are consistent with one another [15–18], and so these data can be adopted for constraining the WF parameters. Based on the present DA model, the model parameter B for $\phi_\pi(x, \mu^2)$ can be determined, and then one can predict the behavior of the pion-photon TFF in high- Q^2 regions, which can be tested in the future experiments.

The remaining parts of the paper are organized as follows. In Sec. II, we give a brief review on the pion leading-twist WF/DA and properties of the DA are also presented. In Sec. III we show how DA parameters can be constrained, and present a detailed derivation of the parameter B by using the $B/D \rightarrow \pi$ transition form factors within the light-cone sum rule (LCSR). A discussion on the pion-photon TFF and $B^0 \rightarrow \pi^0\pi^0$ process is presented in Sec. V. The final section is reserved for a summary.

II. A BRIEF REVIEW ON THE PION LEADING-TWIST WF/DA

One useful way of modeling the hadronic valence WF is to use the approximate bound-state solution of a hadron in

terms of the quark model as the starting point. The Brodsky-Huang-Lepage prescription [19] of the hadronic WF is rightly obtained in this way by connecting the equal-time WF in the rest frame and the WF in the infinite-momentum frame. Based on this prescription, the revised light-cone harmonic oscillator model of the pion leading-twist WF was suggested in Refs. [12,13], which reads

$$\Psi_\pi(x, \mathbf{k}_\perp) = \sum_{\lambda_1, \lambda_2} \chi^{\lambda_1, \lambda_2}(x, \mathbf{k}_\perp) \Psi_\pi^R(x, \mathbf{k}_\perp), \quad (4)$$

where $\chi^{\lambda_1, \lambda_2}(x, \mathbf{k}_\perp)$ stands for the spin-space WF, and λ_1 and λ_2 are the helicity states of the two constitute quarks in the pion. The $\chi^{\lambda_1, \lambda_2}(x, \mathbf{k}_\perp)$ comes from the Wigner-Melosh rotation whose explicit form can be found in Refs. [20,21]. $\Psi_\pi^R(x, \mathbf{k}_\perp)$ indicates the spatial WF, which can be divided into a \mathbf{k}_\perp -dependent part and an x -dependent part. For the \mathbf{k}_\perp -dependent part, Brodsky, Huang, and Lepage suggested that there is a possible connection between the rest frame WF $\Psi_{\text{c.m.}}(\mathbf{q})$ and the light-cone WF $\Psi_{\text{LC}}(x, \mathbf{k}_\perp)$ [19],

$$\Psi_{\text{c.m.}}(\mathbf{q}^2) \leftrightarrow \Psi_{\text{LC}} \left[\frac{\mathbf{k}_\perp^2 + m_q^2}{4x(1-x)} - m_q^2 \right], \quad (5)$$

where m_q stands for the mass of the constitute quarks. From an approximate bound-state solution in the quark models for the pion, the WF of the harmonic oscillator model in the rest frame can be obtained [22]. Thus, for the \mathbf{k}_\perp -dependent part of the spatial WF $\Psi_\pi^R(x, \mathbf{k}_\perp)$, we have

$$\Psi_\pi^R(x, \mathbf{k}_\perp) \propto \exp \left[-\frac{\mathbf{k}_\perp^2 + m_q^2}{8\beta^2 x(1-x)} \right]. \quad (6)$$

For the x -dependent part of $\Psi_\pi^R(x, \mathbf{k}_\perp)$, we take $\varphi_\pi(x) = [1 + B \times C_2^{3/2}(2x-1)]$, which dominates the longitudinal distribution broadness of the WF and can be expanded in Gegenbauer polynomials. Here we only keep the first two terms in $\varphi_\pi(x)$, in which the parameter $B \sim a_2$ can be regarded as an effective parameter to determine the broadness of the longitudinal part of the WF.

As a combination, the explicit form of the spatial WF can be obtained as

$$\Psi_\pi^R(x, \mathbf{k}_\perp) = A \varphi_\pi(x) \exp \left[-\frac{\mathbf{k}_\perp^2 + m_q^2}{8\beta^2 x(1-x)} \right], \quad (7)$$

where A is the normalization constant. After integration over the transverse-momentum dependence, one can obtain the pion DA with the help of Eq. (3),

$$\begin{aligned} \phi_\pi(x, \mu_0^2) &= \frac{\sqrt{3} A m_q \beta}{2\pi^{3/2} f_\pi} \sqrt{x(1-x)} \varphi_\pi(x) \\ &\times \left\{ \text{Erf} \left[\sqrt{\frac{m_q^2 + \mu_0^2}{8\beta^2 x(1-x)}} \right] \right. \\ &\left. - \text{Erf} \left[\sqrt{\frac{m_q^2}{8\beta^2 x(1-x)}} \right] \right\}, \quad (8) \end{aligned}$$

where $\text{Erf}(x) = \frac{2}{\sqrt{\pi}} \int_0^x e^{-t^2} dt$.

Except for the constituent quark mass m_q , which can be taken to have the conventional value of about 0.30 GeV, there are three undetermined parameters— A , β and B —in the above model. Two important constraints for these parameters have been found in Ref. [19]: 1) the process $\pi \rightarrow \mu \bar{\nu}$ provides the WF normalization condition

$$\int_0^1 dx \int \frac{d^2 \mathbf{k}_\perp}{16\pi^3} \Psi_\pi(x, \mathbf{k}_\perp) = \frac{f_\pi}{2\sqrt{6}}; \quad (9)$$

2) the sum rule derived from the $\pi^0 \rightarrow \gamma\gamma$ decay amplitude implies

$$\int_0^1 dx \Psi_\pi(x, \mathbf{k}_\perp = \mathbf{0}) = \frac{\sqrt{6}}{f_\pi}. \quad (10)$$

In addition to these two basic constraints, one needs other processes involving pions to further constrain the parameters, especially to determine the value of the parameter B . We present the DAs for $B = 0.00, 0.30$, and 0.60 in Fig. 1, where, as a comparison, the asymptotic DA and CZ-DA are also shown. When the value of B changes from 0.00 to 0.60, together with the constraints (9) and (10), the pion DA model can mimic the DA shapes from asymptotic-like to CZ-like:

- (i) The second moments a_2 vary from 0.03 to 0.68.
- (ii) The first inverse moments of the pion DA at energy scale μ_0 , $\int_0^1 [\phi_\pi(x, \mu_0^2)/x] dx$, vary from 3.0 to 5.0. Thus, if we have precise measurements for certain processes, then by comparing the theoretical estimations derived under the DA model (8) one can conveniently fix the pion DA behavior.

We put the WF parameters for several typical values of B in Table I, where the region of the parameter B is broadened to be $[-0.60, 0.60]$. The value of B is close to the second Gegenbauer moment, $B \sim a_2$, and because of the

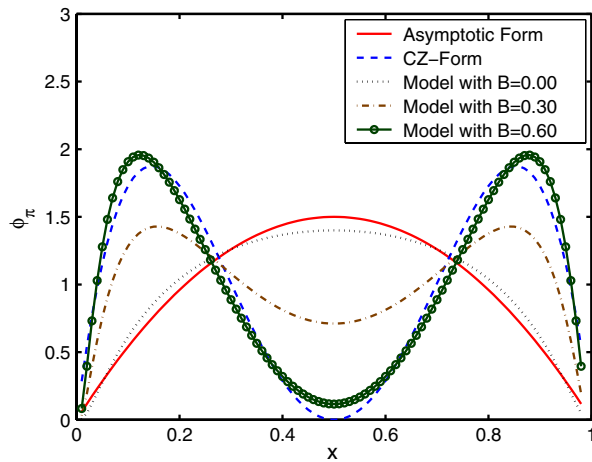


FIG. 1 (color online). The pion DA model $\phi_\pi(x, \mu_0^2)$ defined in Eq. (8) versus the parameter B [12]. By varying B from 0.00 to 0.60, $\phi_\pi(x, \mu_0^2)$ changes from asymptotic-like to CZ-like.

TABLE I. Typical pion WF parameters with $m_q = 0.30$ GeV and $\mu_0 = 1$ GeV. The second and fourth Gegenbauer moments are also presented.

| B | A (GeV $^{-1}$) | β (GeV) | $a_2(\mu_0^2)$ | $a_4(\mu_0^2)$ |
|-------|--------------------|---------------|----------------|----------------|
| -0.60 | 36.03 | 0.456 | -0.523 | 0.051 |
| -0.30 | 30.43 | 0.514 | -0.279 | 0.000 |
| 0.00 | 24.80 | 0.589 | 0.028 | -0.027 |
| 0.30 | 20.05 | 0.672 | 0.364 | -0.017 |
| 0.60 | 16.46 | 0.749 | 0.681 | 0.022 |

fact that the longitudinal distribution is dominated by the second Gegenbauer moment (cf. Refs. [5,9,23–26]) the parameter B dominantly determines the broadness of the longitudinal part of the wave function.

The parameters listed in Table I are for $\mu_0 = 1$ GeV. They can be run to any other scales by applying the evolution equation, i.e., to order $\mathcal{O}(\alpha_s)$, we have [5]

$$x_1 x_2 \frac{\partial \tilde{\phi}_\pi(x_i, \mu^2)}{\partial \ln \mu^2} = C_F \frac{\alpha_s(\mu^2)}{4\pi} \left\{ \int_0^1 [dy] V(x_i, y_i) \tilde{\phi}_\pi(y_i, \mu^2) - x_1 x_2 \tilde{\phi}_\pi(x_i, \mu^2) \right\}, \quad (11)$$

where $[dy] = dy_1 dy_2 \delta(1 - y_1 - y_2)$, $\phi_\pi(x_i, \mu^2) = x_1 x_2 \tilde{\phi}_\pi(x_i, \mu^2)$, and

$$V(x_i, y_i) = 2 \left[x_1 y_2 \theta(y_1 - x_1) \left(\delta_{h_1 h_2} + \frac{\Delta}{(y_1 - x_1)} \right) + (1 \leftrightarrow 2) \right].$$

The θ function is the usual step function, the color factor $C_F = 4/3$, $\delta_{h_1 h_2} = 1$ when the q and \bar{q} helicities are opposite, and $\Delta \tilde{\phi}_\pi(y_i, \mu^2) = \tilde{\phi}_\pi(y_i, \mu^2) - \tilde{\phi}_\pi(x_i, \mu^2)$.

Practically, the above evolution (11) can be solved by using the DA Gegenbauer expansion (1), which transforms the DA scale dependence to the determination of the scale dependence of the Gegenbauer moments [3,4]. More explicitly, the explicit expression for $a_n(\mu^2)$ to leading-logarithmic accuracy can be written as [27]

$$a_n(\mu^2) = a_n(\mu_0^2) \left(\frac{\alpha_s(\mu^2)}{\alpha_s(\mu_0^2)} \right)^{\gamma_n/\beta_0}, \quad (12)$$

where the anomalous dimensions

$$\gamma_n = C_F \left(1 - \frac{2}{(n+1)(n+2)} + 4 \sum_{m=2}^{n+1} \frac{1}{m} \right) \quad (13)$$

with $\beta_0 = (11N_c - 2N_f)/3$. Usually, one truncates the Gegenbauer expansion with the first several terms ($n = 0, 2, 4, 6$, respectively) to derive the DA behavior at the high-energy scales.

In this paper we solve the evolution equation (11) to get the DAs' behavior at the higher-energy scale. It is noted that if the Gegenbauer expansion converges quickly, these two evolution methods (11) and (12) are equivalent to each

TABLE II. Typical pion WF parameters for $m_q = 0.30$ GeV at several typical energy scales, $\mu = 1, 1.5$, and 3 GeV, respectively.

| A (GeV $^{-1}$) | $\mu = 1$ GeV | | $\mu = 1.5$ GeV | | | $\mu = 3$ GeV | | |
|--------------------|---------------|---------------|--------------------|-------|---------------|--------------------|-------|---------------|
| | B | β (GeV) | A (GeV $^{-1}$) | B | β (GeV) | A (GeV $^{-1}$) | B | β (GeV) |
| 24.63 | 0.01 | 0.592 | 24.99 | 0.037 | 0.560 | 25.11 | 0.033 | 0.556 |
| 23.93 | 0.05 | 0.603 | 24.40 | 0.073 | 0.567 | 24.63 | 0.062 | 0.562 |
| 23.09 | 0.10 | 0.617 | 23.67 | 0.118 | 0.577 | 24.05 | 0.099 | 0.570 |
| 22.44 | 0.14 | 0.628 | 23.11 | 0.154 | 0.585 | 23.59 | 0.128 | 0.576 |
| 22.28 | 0.15 | 0.631 | 22.97 | 0.163 | 0.587 | 23.48 | 0.135 | 0.578 |
| 21.50 | 0.20 | 0.645 | 22.30 | 0.208 | 0.597 | 22.93 | 0.171 | 0.585 |
| 20.76 | 0.25 | 0.658 | 21.65 | 0.252 | 0.607 | 22.39 | 0.207 | 0.593 |
| 20.05 | 0.30 | 0.672 | 21.03 | 0.296 | 0.617 | 21.88 | 0.242 | 0.601 |
| 19.37 | 0.35 | 0.686 | 20.43 | 0.340 | 0.626 | 21.38 | 0.277 | 0.608 |
| 18.72 | 0.40 | 0.699 | 19.87 | 0.383 | 0.636 | 20.90 | 0.311 | 0.616 |
| 18.47 | 0.42 | 0.704 | 19.65 | 0.400 | 0.640 | 20.72 | 0.325 | 0.618 |

other. The solution of the evolution equation (11) can be done numerically. Here we suggest an equivalent but simpler and more effective way to get the DA after evolution, i.e., we transform the whole scale dependence of $\phi_\pi(x, \mu_0^2)$ into the scale dependence of the undetermined parameters A , B , and β . The valence-quark mass m_q is scale independent and we keep it to be 0.30 GeV. The main idea is to take the second Gegenbauer moment $a_2(\mu^2)$ as a ligament between the DA and the DA parameters. Firstly, from the initial DA $\phi_\pi(x, \mu_0^2)$ with known A , B , and β at the initial μ_0 , we derive its second Gegenbauer moment $a_2(\mu_0^2)$ via Eq. (2), and get its value at any scale μ by using the evolution equation (12). Secondly, we use the value of $a_2(\mu^2)$ together with the two constraints (9) and (10) to determine the values of A , β , and B at the scale μ . We put the parameters A , B , and β at three typical scales— $\mu = 1, 1.5$, and 3 GeV—which are shown in Table II. From the table, one observes that the value of A increases and the value of β decreases as we move along the scale.

III. DETERMINATION OF DA FROM $B/D \rightarrow \pi$ TRANSITION FORM FACTORS

The semileptonic B -meson decay $B \rightarrow \pi l \nu$ is usually used to extract the Cabibbo-Kobayashi-Maskawa (CKM) matrix element $|V_{ub}|$, whose differential cross section for massless leptons can be written as

$$\begin{aligned} \frac{d\Gamma}{dq^2}(B \rightarrow \pi l \nu) &= \frac{C_F^2 |V_{ub}|^2}{192 \pi^3 m_B^3} [(q^2 + m_B^2 - m_\pi^2)^2 - 4m_B^2 m_\pi^2]^{3/2} |f_+^{B \rightarrow \pi}(q^2)|^2, \\ & \quad (14) \end{aligned}$$

where the momentum transfer $q = p_B - p_\pi$. The TFF $f_+^{B \rightarrow \pi}$ is the key factor of the process, which has been deeply investigated by using several approaches, such as the pQCD approach [28,29], the QCD LCSR approach [23–25,27,30–36], and the lattice QCD approach [37,38].

Different approaches are applicable for different energy regions. Among them, the QCD LCSR is reliable for the intermediate energy region, which can be extended to the whole physical region with proper extrapolation. So this approach is usually adopted for a detailed analysis in comparison with the experimental data.

Under LCSR, the expression for $f_+^{B \rightarrow \pi}$ depends on how one chooses the correlator [39]: different choices of the currents in the correlation function shall result in different expressions, in which the pionic different-twist structures provide different contributions. Here we adopt the chiral correlator suggested in Ref. [31] for our discussion, in which the leading-twist DA's contribution has been amplified in order to provide us with a better chance to know the detail of the leading-twist DA in comparison with data. By using the chiral correlator, up to twist-4, the form factor $f_+^{B \rightarrow \pi}(0)$ in the large-recoil region can be obtained as [35]

$$\begin{aligned} f_B f_+^{B \rightarrow \pi}(0) e^{-\frac{m_B^2}{M^2}} &= -\frac{m_b^2 f_\pi}{2\pi m_B^2} \int_{m_b^2}^{s_0^B} ds e^{-\frac{s}{M^2}} \frac{1}{s} \\ &\times \int_0^{s/m_b^2} d\eta \text{Im}T\left(\frac{m_b^2}{s}, \eta, \frac{s}{m_b^2}, \mu\right) \phi_\pi\left(\frac{m_b^2}{s}, \eta, \mu\right) \\ &+ \frac{f_\pi}{m_B^2} \int_{u_0}^1 du e^{-\frac{m_b^2}{uM^2}} \left[-\frac{u}{4} \frac{d^2 \phi_{4\pi}(u)}{du^2} + u \psi_{4\pi}(u) \right. \\ &\left. + \int_0^u dv \psi_{4\pi}(v) - \frac{d}{du} I_{4\pi}(u) \right], \quad (15) \end{aligned}$$

where f_B , m_B , M^2 , m_b , and s_0^B indicate the B -meson decay constant, the B -meson mass, the Borel parameter, the b -quark mass, and the effective threshold parameter, respectively. The parameter $u_0 = m_b^2/s_0^B$. The functions $\phi_{4\pi}$ and $\psi_{4\pi}$ are pion two-particle twist-4 DAs. $I_{4\pi}$ is a combination of pion three-particle twist-4 DAs. The hard-scattering amplitude $\text{Im}T(\eta m_b^2/s, s/m_b^2, \mu)$ involves the leading-order (LO) and next-to-leading-order (NLO) parts.

The scale of the process $\mu = \sqrt{m_B^2 - m_b^2} \simeq 3$ GeV.

Furthermore, the semileptonic D -meson decay $D \rightarrow \pi l \nu$ can also be used to extract the CKM matrix element V_{cd} if we know the $D \rightarrow \pi$ TFF $f_+^{D \rightarrow \pi}$ well. The TFF $f_+^{D \rightarrow \pi}$ has been studied in Refs. [35,40,41]. By replacing all the B -meson parameters in Eq. (15) with those of the D meson, we can obtain the LCSR expression for $f_+^{D \rightarrow \pi}(0)$. For example, the scale for $f_+^{B \rightarrow \pi}$ is now $\mu = \sqrt{m_D^2 - m_c^2} \simeq 1.5$ GeV.

Using the formula (15), we find that the contributions from the pion twist-4 DA terms are less than 1% for $f_+^{B \rightarrow \pi}(0)$ and less than 5% for $f_+^{D \rightarrow \pi}(0)$. Thus this provides a good platform to study the properties of the pion leading-twist DA. In Ref. [39], the authors have made use of this platform to determine the DA parameter B with experimental data of $f_+^{B \rightarrow \pi} |V_{ub}|$ by taking the input parameters the same as those in Ref. [35]. In this present section, we update their analysis by using the input parameters from the Particle Data Group (PDG) [42], and simultaneously we make use of $f_{D^+} f_+^{D \rightarrow \pi}(0)$ as a further constraint to determine the pion DA parameters.

The input parameters are the following. The \overline{MS} -running b and c masses and the B^+ - and D^+ -meson masses are [42] $\bar{m}_b(\bar{m}_b) = 4.18 \pm 0.03$ GeV, $\bar{m}_c(\bar{m}_c) = 1.275 \pm 0.025$ GeV, $m_{B^+} = 5279.25 \pm 0.17$ MeV and $m_{D^+} = 1869.62 \pm 0.15$ MeV, respectively. The B^+ -meson decay constant $f_{B^+} = 214_{-7}^{+5}$ MeV [24]. Because there is a large discrepancy for the estimation of the D^+ -meson decay constant f_{D^+} [43–47], instead of using $f_+^{D \rightarrow \pi}(0)$ as a criteria we adopt the combined value of $f_{D^+} f_+^{D \rightarrow \pi}(0)$ to constrain the pion DA. The pion decay constant f_{π^0} is set to be f_{π^+} [48], which is $130.41 \pm 0.03 \pm 0.20$ MeV [42]. As for the effective threshold and Borel variables, we take them to be same as those in Ref. [35].

Experimentally, from the processes $B^+ / D^+ \rightarrow \pi^0 l^+ \nu_l$, it has been shown by the *BABAR* [49] and *CLEO* [50] collaborations that the multiplication of the form factor and the corresponding CKM matrix element are

$$f_+^{B \rightarrow \pi}(0) |V_{ub}| = (9.4 \pm 0.3 \pm 0.3) \times 10^{-4} \quad (16)$$

and

$$f_+^{D \rightarrow \pi}(0) |V_{cd}| = 0.146 \pm 0.007 \pm 0.002. \quad (17)$$

From a simultaneous fit to the experimental partial rates and lattice points on the exclusive process $B \rightarrow \pi l \nu$ versus q^2 , the CKM matrix element $|V_{ub}|$ is derived as $(3.23 \pm 0.31) \times 10^{-3}$ [38]. As a combination, we can obtain the experimental value for $f_+^{B \rightarrow \pi}(0)$,

$$f_+^{B \rightarrow \pi}(0) = 0.291_{-0.009}^{+0.010}. \quad (18)$$

Comparing this value with the estimated one from the LCSR (15), as indicated by Fig. 2, we obtain the first reasonable region for the parameter B ,

$$B_{(B \rightarrow \pi l \nu)} = [0.01, 0.42], \quad (19)$$

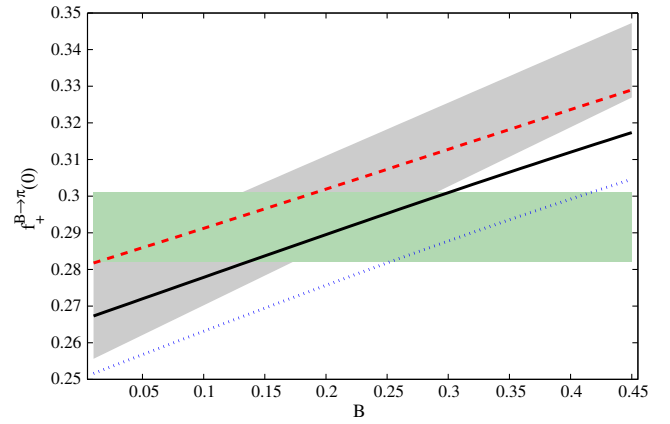


FIG. 2 (color online). The value of $f_+^{B \rightarrow \pi}(0)$ versus the DA parameter B . The solid, dashed, and dotted lines stand for the central, upper, and lower values obtained from the LCSR (15) with the leading-twist DA model (8), respectively. The lighter shaded band indicates the experimental band (18). The thicker shaded band is the result of Ref. [39].

where all the input parameters are varied within their reasonable regions listed above. Our present value for B is different from that of Ref. [35], which is due to the fact that we have adopted a different \overline{MS} b -quark mass. Figure 2 shows the value of $f_+^{B \rightarrow \pi}(0)$ versus the parameter B . Where the lighter shaded band indicates the experimental value (18), the solid, dashed, and dotted lines stand for the central, upper, and lower ones calculated by the LCSR (15), respectively, and the thicker shaded band is the result of Ref. [39].

For the D -meson case, whose lifetime is 1040 ± 7 fs [51], we can adopt the measurement of $\mathcal{B}(D^+ \rightarrow \mu^+ \nu)$. Then, using the formulas

$$\Gamma(D^+ \rightarrow l^+ \nu) = \frac{C_F^2}{8\pi} f_{D^+}^2 m_l^2 m_{D^+} \left(1 - \frac{m_l^2}{m_{D^+}^2}\right)^2 |V_{cd}|^2,$$

where m_l is the mass of the lepton, we can inversely obtain

$$f_{D^+} |V_{cd}| = 46.4 \pm 2.0 \text{ MeV}. \quad (20)$$

Furthermore, by using the PDG value for $|V_{cd}| = 0.230 \pm 0.011$ [42], together with Eqs. (17) and (20), we can obtain an experimental constraint for the multiplication of f_{D^+} with $f_+^{D \rightarrow \pi}(0)$, i.e.,

$$f_{D^+} f_+^{D \rightarrow \pi}(0) = 0.128 \pm 0.012 \text{ GeV}. \quad (21)$$

Combining this experimental value [Eq. (21)] for $f_{D^+} f_+^{D \rightarrow \pi}(0)$ with the theoretical one calculated by sum rules [Eq. (15)], as shown in Fig. 3, we obtain the second reasonable region for the parameter B ,

$$B_{(D \rightarrow \pi l \nu)} = [0.00, 0.14]. \quad (22)$$

Figure 3 shows the value of $f_{D^+} f_+^{D \rightarrow \pi}(0)$ versus the parameter B , where the shaded band indicates the experimental values [Eq. (21)] and the solid, dashed, and dotted

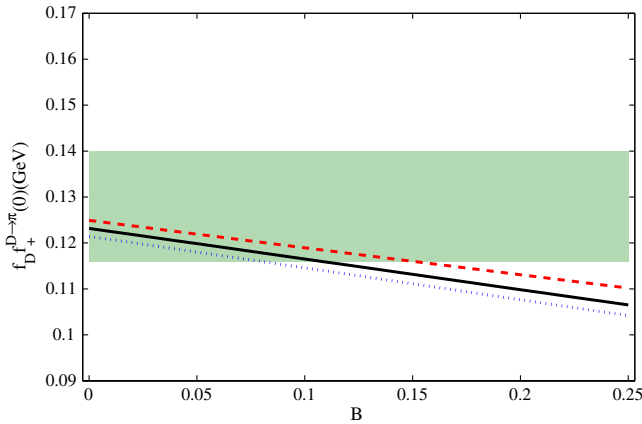


FIG. 3 (color online). The value of $f_{D^+}^{D \to \pi}(0)$ versus the parameter B . The solid, dashed, and dotted lines stand for the central, upper, and lower values calculated by the LCSR (15), respectively (with parameter changes for the D -meson case). The shaded band indicates the experimental value (21) of $f_{D^+}^{D \to \pi}(0)$.

lines stand for the central, upper, and lower edge of the theoretical values calculated by the LCSR (15), respectively, with slight parameter changes to agree with the D -meson case. Here we have implicitly set the value of B to be bigger than 0, which is reasonable, since—as shown in Fig. 1—by varying $B \in [0, 0.6]$ the DA can mimic all of its known behaviors suggested in the literature.

As a final remark, the D -meson mass may not be large enough; the energy scale is about 1.5 GeV, and thus the reliability of the LCSR for the form factor $f_{D^+}^{D \to \pi}$ may be less reliable than in the B -meson case. So we give two schemes for setting the region of parameter B .

- (i) Scheme A: If we believe that the LCSR has the same importance as that of $B \rightarrow \pi l \nu$, then the range of B is

$$B = [0.01, 0.14]. \quad (23)$$

- (ii) Scheme B: If only the LCSR for $B \rightarrow \pi l \nu$ is acceptable, we have a broader region, as shown in Eq. (19).

IV. DISCUSSION

If the parameter B is determined, the shape of the pion leading-twist DA can be fixed. Under scheme A, the second and fourth moments of the pion twist-2 DA can be calculated as $a_2(1 \text{ GeV}) = [0.039, 0.184]$ and $a_4(1 \text{ GeV}) = [-0.027, -0.028]$, respectively. Under scheme B, the first two moments change to $a_2(1 \text{ GeV}) = [0.039, 0.495]$ and $a_4(1 \text{ GeV}) = [-0.027, -0.004]$. We present our DA model with different values of B at $\mu = 1 \text{ GeV}$ in Fig. 4, where the thin-solid, dashed, dotted, dash-dotted, and thick-solid lines are for $B = 0.01, 0.14, 0.2, 0.3,$ and 0.42 , respectively.

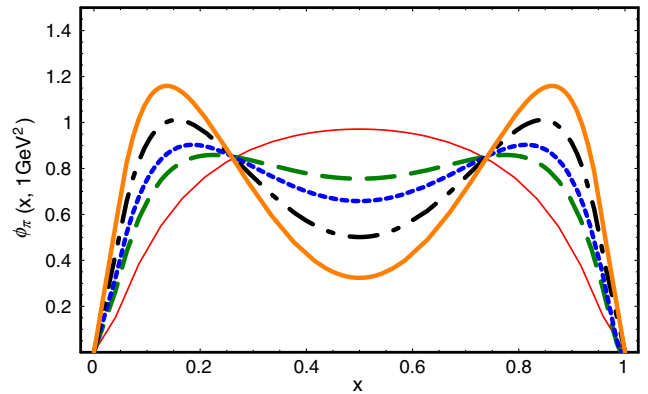


FIG. 4 (color online). The pion leading-twist DA versus the parameter B at $\mu = 1 \text{ GeV}$, where the thin-solid, dashed, dotted, dash-dotted, and thick-solid lines are $B = 0.01, 0.14, 0.2, 0.3,$ and 0.42 , respectively.

As two applications, we use our pion leading-twist DA to deal with the pion-photon TFF $F_{\pi\gamma}(Q^2)$ and the branching ratio of the B -meson exclusive decay $B^0 \rightarrow \pi^0 \pi^0$.

A. The pion-photon TFF $F_{\pi\gamma}(Q^2)$

As a first application, we revisit the pion-photon TFF. The pion-photon TFF provides the simplest example for the perturbative analysis to exclusive processes, which has aroused great interest since it was first analyzed by Lepage and Brodsky [5]. Subsequently, to explain the abnormal large- Q^2 behavior observed by the *BABAR* Collaboration in 2009 [17], many analyses were done, e.g., using the perturbative QCD approach [12,13,52,53] or the LCSR approach [54–56]. However, last year the Belle Collaboration released their new analysis [18], which dramatically differed from that of the *BABAR* Collaboration; however, it is likely to agree with the asymptotic behavior estimated by Ref. [5]. Many attempts have been made to clarify the situation [14,39,57–60].

Following the idea suggested by Ref. [61], we have studied the pion-photon TFF with the pQCD approach by carefully dealing with the transverse-momentum corrections [1,12–14]. Generally, the pion-photon TFF $F_{\pi\gamma}(Q^2)$ can be written as a sum of the valence-quark part $F_{\pi\gamma}^{(V)}(Q^2)$ and the non-valence-quark part $F_{\pi\gamma}^{(NV)}(Q^2)$,

$$F_{\pi\gamma}(Q^2) = F_{\pi\gamma}^{(V)}(Q^2) + F_{\pi\gamma}^{(NV)}(Q^2). \quad (24)$$

The valence-quark part $F_{\pi\gamma}^{(V)}(Q^2)$ indicates the pQCD-calculable leading Fock-state contribution, e.g., the direct annihilation of the valence $q\bar{q}$ pair into two photons, which dominates the TFF when Q^2 is large. The non-valence-quark part $F_{\pi\gamma}^{(NV)}(Q^2)$ is related to the nonperturbative higher Fock-state contributions, which can be estimated via a proper phenomenological model. The analytic expressions for $F_{\pi\gamma}^{(V)}(Q^2)$ and $F_{\pi\gamma}^{(NV)}(Q^2)$ can be found in Ref. [12].

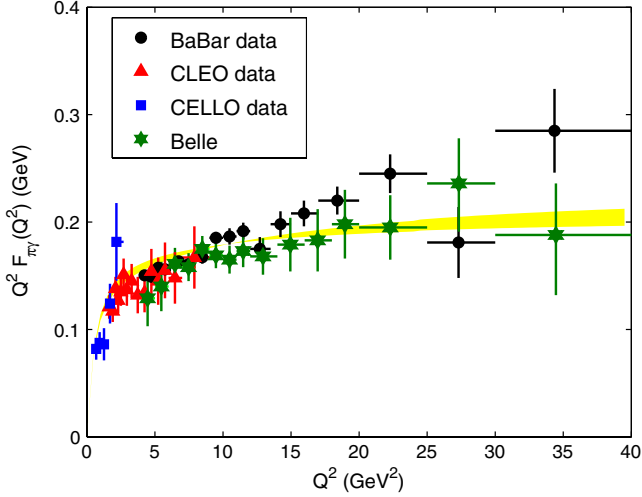


FIG. 5 (color online). $Q^2 F_{\pi\gamma}(Q^2)$ with our WF model [Eqs. (4) and (7)], varying the model parameter B within the region $[0.01, 0.14]$. The shaded band is our theoretical estimation.

Taking all of the input parameters to be the same as those in Ref. [12], but with our present DA model with $B \in [0.01, 0.14]$, we show the pion-photon TFF $F_{\pi\gamma}(Q^2)$ in Fig. 5. The upper and lower borderlines correspond to $B = 0.01$ and 0.14 , respectively. The figure shows that in the small- Q^2 region, $Q^2 \lesssim 15 \text{ GeV}^2$, the pion-photon TFF can explain the CELLO [15], CLEO [16], BABAR [17], and Belle [18] experimental data simultaneously, while for the large- Q^2 region, our present estimation favors the Belle data and disfavors the BABAR data. This result is in agreement with the conclusion of Refs. [58,60]. If we take $B \in [0.01, 0.42]$, the calculated curve for the pion-photon TFF with the upper limit of the parameter ($B = 0.42$) will be between the Belle and BABAR data.

B. The B -meson exclusive decay $B^0 \rightarrow \pi^0 \pi^0$

As a second application, we discuss the process $B^0 \rightarrow \pi^0 \pi^0$, which has been calculated within the pQCD approach [62–67]. At present, we adopt the same calculation technology as described in Refs. [64–67] to do our calculation. The corresponding decay width can be written as

$$\Gamma(B^0 \rightarrow \pi^0 \pi^0) = \frac{C_F^2 M_B^2}{128\pi} |V_{ub}^* V_{ud} M_a^T|^2 [1 + z^2 + 2z \cos(\delta - \gamma)], \quad (25)$$

where $V_{ub} \simeq |V_{ub}| e^{-i\gamma}$, $z = |V_{tb}^* V_{td} / V_{ub}^* V_{ud}| |M_a^P / M_a^T|$, δ is the relative strong phase between tree diagrams (M_a^T) and penguin diagrams (M_a^P), and γ is the CKM phase angle. The specific corresponding formulas can be found in Ref. [67].

In doing the numerical calculation, we adopt the same B -meson DA and pion twist-3 DAs used in Ref. [67], but

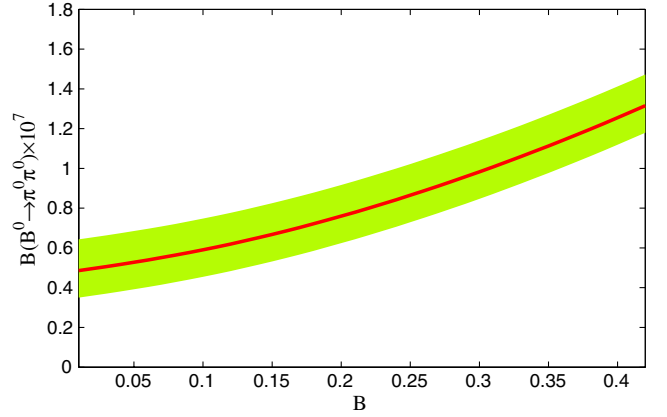


FIG. 6 (color online). The branching ratio $\mathcal{B}(B^0 \rightarrow \pi^0 \pi^0)$ for the exclusive process $B^0 \rightarrow \pi^0 \pi^0$ versus the parameter B . The red solid line indicates the central value of $\mathcal{B}(B^0 \rightarrow \pi^0 \pi^0)$, and the shaded band stands for the uncertainty from the dominant uncertainty sources, such as m_0 , γ , $|V_{ub}|$, and f_B .

with our present pion leading-twist DA. The result is shown in Fig. 6, where we vary the parameter B within the region $[0.01, 0.42]$, and the shaded band indicates the uncertainty from the dominant uncertainty sources, such as $m_0 = 1.6 \pm 0.2 \text{ GeV}$ [68], $\gamma = 68_{-11}^{\circ} + 10^{\circ}$ [42], $|V_{ub}|$, and f_B . Other parameters are taken at their central values as reported by the Particle Data Group [42]—e.g., $|V_{td}| = 0.00867$, $|V_{tb}| = 0.999146$, $|V_{ud}| = 0.97427$, $m_{B^0} = 5279.58 \text{ MeV}$, $m_{\pi^0} = 134.9766 \text{ MeV}$ —due to the fact that their uncertainties are comparatively small. Moreover, we take $\Lambda_{\text{QCD}}^{f=4} = 0.25 \text{ GeV}$ as in Ref. [67]. The branching ratio $\mathcal{B}(B^0 \rightarrow \pi^0 \pi^0)$ increases with the parameter B , i.e., the value of $\mathcal{B}(B^0 \rightarrow \pi^0 \pi^0)$ increases and approaches the experimental data for larger values of B . This agrees with the behavior of the pion leading-twist DA shown in Fig. 4. Figure 4 shows that the pion leading-twist DA in the region close to the end point becomes larger when the parameter B is bigger, and correspondingly the obtained branching ratio $\mathcal{B}(B^0 \rightarrow \pi^0 \pi^0)$ becomes larger. This situation does not imply that there is an end-point singularity for our modal DA. For the twist-3 contributions, because of the inclusion of the k_T -dependent terms [64,69], our calculation also has no end-point singularity.

Our present estimation, $\mathcal{B}(B^0 \rightarrow \pi^0 \pi^0) \sim [0.35, 1.47] \times 10^{-7}$, is much smaller than the experimental data $(1.62 \pm 0.31) \times 10^{-6}$ [42]. The reason lies in the following. 1) we only take the LO contribution into consideration. At present, we mostly care about the influence from the twist-2 DA model parameter B , and do not expect to solve the puzzle of why there is a tremendous difference between the experimental data and the theoretical estimation. 2) As indicated by Refs. [70–73], some important factors may need to be considered in the calculation, such as that the NLO correction may be big or there may be large nonperturbative contributions, or even that an unknown

mechanism may exist, which is beyond the scope of the present paper.

V. SUMMARY

In the present paper, based on the revised light-cone harmonic oscillator model for the pion leading-twist DA, we have made a combined analysis of the pion DA by using the channels $\pi^0 \rightarrow \gamma\gamma$, $\pi \rightarrow \mu\bar{\nu}$, and the semileptonic decays $B \rightarrow \pi l\nu$ and $D \rightarrow \pi l\nu$ in comparison with the experimental data. Based on the constraints from these processes, typical parameters for the pion leading-twist DA are presented in Table II.

In addition to the two constraints (9) and (10), by using the constraint from the process $B \rightarrow \pi l\nu$, the parameter B is restricted to the region $[0.01, 0.42]$. If we use the process $D \rightarrow \pi l\nu$ as a further constraint, we can obtain a more narrow region, $B = [0.00, 0.14]$. Using the pion leading-twist DA model, we recalculated the branching ratio $\mathcal{B}(B^0 \rightarrow \pi^0\pi^0)$ and the pion-photon TFF. The branching ratio $\mathcal{B}(B^0 \rightarrow \pi^0\pi^0)$ increases with the parameter B . For the pion-photon TFF, our present result with the parameter

$B = [0.01, 0.14]$ favors the Belle data and the corresponding pion DA is slightly different from the asymptotic form. One can then predict the behavior of the pion-photon TFF in high- Q^2 regions, which can be tested in the future experiments. It is expected that *BABAR* and Belle can obtain more accurate and consistent data in the future; then, the behavior of the pion DA can be more completely determined. On the other hand, we can adopt more pionic processes—such as the pion electromagnetic form factor—to impose a further constraint on the pion DA, which is in progress. It is believed that the pion DA will be determined by the global fit to the exclusive processes involving the pion in the near future.

ACKNOWLEDGMENTS

The authors would like to thank Zuo-Hong Li, Nan Zhu, and Zhi-Tian Zou for helpful discussions. This work was supported in part by the Natural Science Foundation of China under Grant Nos. 11235005 and No. 11075225, and by the Program for New Century Excellent Talents in University under Grant No. NCET-10-0882.

-
- [1] T. Huang and X. G. Wu, *Int. J. Mod. Phys. A* **22**, 3065 (2007).
 - [2] I. V. Musatov and A. V. Radyushkin, *Phys. Rev. D* **56**, 2713 (1997).
 - [3] G. P. Lepage and S. J. Brodsky, *Phys. Lett.* **87B**, 359 (1979).
 - [4] A. V. Efremov and A. V. Radyushkin, *Phys. Lett.* **94B**, 245 (1980).
 - [5] G. P. Lepage and S. J. Brodsky, *Phys. Rev. D* **22**, 2157 (1980).
 - [6] V. L. Chernyak and I. R. Zhitnitsky, *Phys. Rep.* **112**, 173 (1984).
 - [7] X. D. Xiang, X. N. Wang, and T. Huang, *Commun. Theor. Phys.* **6**, 117 (1986); S. V. Mikhailov and A. V. Radyushkin, *Phys. Rev. D* **45**, 1754 (1992); A. P. Bakulev, K. Passek-Kumerički, W. Schroers, and N. G. Stefanis, *Phys. Rev. D* **70**, 033014 (2004).
 - [8] G. Martinelli and C. T. Sachrajda, *Phys. Lett. B* **190**, 151 (1987); T. A. DeGrand and R. D. Loft, *Phys. Rev. D* **38**, 954 (1988); D. Daniel, R. Gupta, and D. G. Richards, *Phys. Rev. D* **43**, 3715 (1991); L. Del Debbio, M. Di Pierro, A. Dougall, and C. Sachrajda (UKQCD Collaboration), *Nucl. Phys. B, Proc. Suppl.* **83**, 235 (2000); L. Del Debbio, M. Di Pierro, and A. Dougall (UKQCD Collaboration), *Nucl. Phys. B, Proc. Suppl.* **119**, 416 (2003).
 - [9] V. L. Chernyak and A. R. Zhitnitsky, *Nucl. Phys.* **B201**, 492 (1982).
 - [10] E. R. Arriola and W. Broniowski, *Phys. Rev. D* **66**, 094016 (2002).
 - [11] J. Botts and G. Sterman, *Nucl. Phys.* **B325**, 62 (1989); T. Huang and Q. X. Shen, *Z. Phys. C* **50**, 139 (1991); H. N. Li and G. Sterman, *Nucl. Phys.* **B381**, 129 (1992).
 - [12] X. G. Wu and T. Huang, *Phys. Rev. D* **82**, 034024 (2010).
 - [13] X. G. Wu and T. Huang, *Phys. Rev. D* **84**, 074011 (2011).
 - [14] X. G. Wu, T. Huang, and T. Zhong, *Chinese Phys. C* **37**, 063105 (2013).
 - [15] H. J. Behrend *et al.* (CELLO Collaboration), *Z. Phys. C* **49**, 401 (1991).
 - [16] V. Savinov *et al.* (CLEO Collaboration), [arXiv:hep-ex/9707028](https://arxiv.org/abs/hep-ex/9707028); J. Gronberg *et al.* (CLEO Collaboration), *Phys. Rev. D* **57**, 33 (1998).
 - [17] B. Aubert *et al.* (*BABAR* Collaboration), *Phys. Rev. D* **80**, 052002 (2009).
 - [18] S. Uehara *et al.* (Belle Collaboration), *Phys. Rev. D* **86**, 092007 (2012).
 - [19] S. J. Brodsky, T. Huang, and G. P. Lepage, in *Proceedings of the Banff Summer Institute, Ban8, Alberta, 1981*, edited by A. Z. Capri and A. N. Kamal (Plenum, New York, 1983), p. 143; G. P. Lepage, S. J. Brodsky, T. Huang, and P. B. Mackenzie, in *Proceedings of the Banff Summer Institute, Ban8, Alberta, 1981*, edited by A. Z. Capri and A. N. Kamal (Plenum, New York, 1983), p. 83; T. Huang, in *Proceedings of XXth International Conference on High Energy Physics, Madison, Wisconsin, 1980*, edited by L. Durand and L. G. Pondrom, AIP Conference Proceedings No. 69 (AIP, New York, 1981), p. 1000.
 - [20] T. Huang, B. Q. Ma, and Q. X. Shen, *Phys. Rev. D* **49**, 1490 (1994).
 - [21] F. G. Cao and T. Huang, *Phys. Rev. D* **59**, 093004 (1999); T. Huang and X. G. Wu, *Phys. Rev. D* **70**, 093013 (2004); X. G. Wu and T. Huang, *Int. J. Mod. Phys. A* **21**, 901 (2006).

- [22] See, e.g., Elementary Particle Theory Group, *Acta Phys. Sin.* **25**, 415 (1976); N. Isgur, in *The New Aspects of Subnuclear Physics*, edited by A. Zichichi (Plenum, New York, 1980), p. 107.
- [23] P. Ball and R. Zwicky, *Phys. Lett. B* **625**, 225 (2005).
- [24] G. Duplancic, A. Khodjamirian, T. Mannel, B. Melic, and N. Offen, *J. High Energy Phys.* **04** (2008) 014.
- [25] A. Khodjamirian, T. Mannel, N. Offen, and Y.-M. Wang, *Phys. Rev. D* **83**, 094031 (2011).
- [26] S. S. Agaev, V. M. Braun, N. Offen, and F. A. Porkert, *Phys. Rev. D* **83**, 054020 (2011).
- [27] P. Ball and R. Zwicky, *Phys. Rev. D* **71**, 014015 (2005).
- [28] M. Wirbel, B. Stech, and M. Bauer, *Z. Phys. C* **29**, 637 (1985); H. N. Li, *Phys. Rev. D* **52**, 3958 (1995); H. N. Li and B. Melić, *Eur. Phys. J. C* **11**, 695 (1999); C. D. Lu, K. Ukai, and M. Z. Yang, *Phys. Rev. D* **63**, 074009 (2001); M. Dahm, R. Jacob, and P. Kroll, *Z. Phys. C* **68**, 595 (1995); A. Szczepaniak, E. M. Henley, and S. J. Brodsky, *Phys. Lett. B* **243**, 287 (1990); Y. Y. Keum, H. N. Li, and A. I. Sunda, *Phys. Rev. D* **63**, 054008 (2001); Z. T. Wei and M. Z. Yang, *Nucl. Phys. B* **642**, 263 (2002); C. D. Lu and M. Z. Yang, *Eur. Phys. J. C* **28**, 515 (2003); D. M. Zeng, X. G. Wu, and Z. Y. Fang, *Chin. Phys. Lett.* **26**, 021401 (2009); W. F. Wang and Z. J. Xiao, *Phys. Rev. D* **86**, 114025 (2012).
- [29] T. Huang and X. G. Wu, *Phys. Rev. D* **71**, 034018 (2005); T. Huang, C. F. Qiao, and X. G. Wu, *Phys. Rev. D* **73**, 074004 (2006).
- [30] V. M. Belyaev, V. M. Braun, A. Khodjamirian, and R. Ruckl, *Phys. Rev. D* **51**, 6177 (1995); P. Ball, *J. High Energy Phys.* **09** (1998) 005; A. Khodjamirian, R. Ruckl, S. Weinzierl, C. W. Winhart, and O. Yakovlev, *Phys. Rev. D* **62**, 114002 (2000); P. Ball and R. Zwicky, *J. High Energy Phys.* **10** (2001) 019.
- [31] T. Huang, Z. H. Li, and X. Y. Wu, *Phys. Rev. D* **63**, 094001 (2001).
- [32] Z. G. Wang, M. Z. Zhou, and T. Huang, *Phys. Rev. D* **67**, 094006 (2003).
- [33] T. Huang, Z. H. Li, X. G. Wu, and F. Zuo, *Int. J. Mod. Phys. A* **23**, 3237 (2008).
- [34] X. G. Wu and T. Huang, *Phys. Rev. D* **79**, 034013 (2009).
- [35] Z. H. Li, N. Zhu, X. J. Fan, and T. Huang, *J. High Energy Phys.* **05** (2012) 160.
- [36] M. Z. Zhou, X. H. Wu, and T. Huang, [arXiv:hep-ph/0402040](https://arxiv.org/abs/hep-ph/0402040); T. Zhong, X. G. Wu, J. W. Zhang, Y. Q. Tang, and Z. Y. Fang, *Phys. Rev. D* **83**, 036002 (2011).
- [37] L. D. Debbio, J. M. Flynn, L. Lellouch, and J. Nieves, *Phys. Lett. B* **416**, 392 (1998); K. C. Bowler, L. Del Debbio, J. M. Flynn, L. Lellouch, V. Lesk, C. M. Maynard, J. Nieves, and D. G. Richards, *Phys. Lett. B* **486**, 111 (2000); D. Becirevic, *Nucl. Phys. B, Proc. Suppl.* **94**, 337 (2001); S. Aoki *et al.* (JLQCD Collaboration), *Phys. Rev. D* **64**, 114505 (2001); E. Gulez, A. Gray, M. Wingate, C. T. H. Davies, G. P. Lepage, and J. Shigemitsu (HPQCD Collaboration), *Phys. Rev. D* **73**, 074502 (2006).
- [38] J. A. Bailey *et al.*, *Phys. Rev. D* **79**, 054507 (2009).
- [39] T. Huang, X. G. Wu, and T. Zhong, *Chin. Phys. Lett.*, **30**, 041201 (2013).
- [40] P. Ball, *Phys. Lett. B* **641**, 50 (2006); A. Khodjamirian, C. Klein, T. Mannel, and N. Offen, *Phys. Rev. D* **80**, 114005 (2009).
- [41] A. Abada, D. Becirevic, Ph. Boucaud, J. P. Leroy, V. Lubicz, and F. Mescia, *Nucl. Phys. B* **619**, 565 (2001); C. Aubin *et al.*, *Phys. Rev. Lett.* **94**, 011601 (2005); C. Bernard *et al.*, *Phys. Rev. D* **80**, 034026 (2009); A. Al-Haydari, A. Ali Khan, V. M. Braun, S. Collins, M. Göckeler, G. N. Lacagnina, M. Panero, A. Schäfer, and G. Schierholz, *Eur. Phys. J. A* **43**, 107 (2010); H. Na, C. T. H. Davies, E. Follana, J. Koponen, G. P. Lepage, and J. Shigemitsu, *Phys. Rev. D* **84**, 114505 (2011); S. Di Vita *et al.*, *Proc. Sci., LAT* (2010) 301.
- [42] J. Beringer *et al.* (Particle Data Group), *Phys. Rev. D* **86**, 010001 (2012).
- [43] C. T. H. Davies, C. McNeile, E. Follana, G. P. Lepage, H. Na, and J. Shigemitsu (HPQCD Collaboration), *Phys. Rev. D* **82**, 114504 (2010); A. Bazavov *et al.* (Fermilab/MILC Collaboration), *Phys. Rev. D* **85**, 114506 (2012).
- [44] B. Blossier *et al.*, *J. High Energy Phys.* **07** (2009) 043.
- [45] J. Bordes, J. Penarrocha, and K. Schilcher, *J. High Energy Phys.* **11** (2005) 014; W. Lucha, D. Melikhov, and S. Simula, *Phys. Lett. B* **701**, 82 (2011).
- [46] A. M. Badalian, B. L. G. Bakker, and Y. A. Simonov, *Phys. Rev. D* **75**, 116001 (2007).
- [47] C. W. Hwang, *Phys. Rev. D* **81**, 054022 (2010).
- [48] K. Kampf and B. Moussallam, *Phys. Rev. D* **79**, 076005 (2009).
- [49] P. del Amo Sanchez *et al.* (BABAR Collaboration), *Phys. Rev. D* **83**, 052011 (2011).
- [50] D. Besson *et al.* (CLEO Collaboration), *Phys. Rev. D* **80**, 032005 (2009); J. Y. Ge *et al.* (CLEO Collaboration), *Phys. Rev. D* **79**, 052010 (2009).
- [51] W.-M. Yao *et al.*, *J. Phys. G* **33**, 1 (2006).
- [52] S. Noguera and V. Vento, *Eur. Phys. J. A* **46**, 197 (2010).
- [53] P. Kroll, *Eur. Phys. J. C* **71**, 1623 (2011).
- [54] S. V. Mikhailov and N. G. Stefanis, *Nucl. Phys. B* **821**, 291 (2009).
- [55] A. P. Bakulev, S. V. Mikhailov, A. V. Pimikov, and N. G. Stefanis, *Phys. Rev. D* **84**, 034014 (2011).
- [56] S. S. Agaev, V. M. Braun, N. Offen, and F. A. Porkert, *Phys. Rev. D* **83**, 054020 (2011).
- [57] S. S. Agaev, V. M. Braun, N. Offen, and F. A. Porkert, *Phys. Rev. D* **86**, 077504 (2012).
- [58] A. P. Bakulev, S. V. Mikhailov, A. V. Pimikov, and N. G. Stefanis, *Phys. Rev. D* **86**, 031501 (2012).
- [59] S. Noguera and V. Vento, *Eur. Phys. J. A* **48**, 143 (2012).
- [60] N. G. Stefanis, A. P. Bakulev, S. V. Mikhailov, and A. V. Pimikov, *Phys. Rev. D* **87**, 094025 (2013).
- [61] F. G. Cao, T. Huang, and B. Q. Ma, *Phys. Rev. D* **53**, 6582 (1996).
- [62] M. Beneke and M. Neubert, *Nucl. Phys. B* **675**, 333 (2003).
- [63] M. Beneke, G. Buchalla, M. Neubert, and C. T. Sachrajda, *Phys. Rev. D* **72**, 098501 (2005).
- [64] H. N. Li, *Phys. Lett. B* **348**, 597 (1995).
- [65] C. D. Lü, K. Ukai, and M. Z. Yang, *Phys. Rev. D* **63**, 074009 (2001).
- [66] C. D. Lü, [arXiv:hep-ph/0110327](https://arxiv.org/abs/hep-ph/0110327).
- [67] Y. Li, C. D. Lü, Z. J. Xiao, and X. Q. Yu, *Phys. Rev. D* **70**, 034009 (2004).

- [68] P. Ball, *J. High Energy Phys.* **01** (1999) 010.
- [69] H.-n. Li and H.L. Yu, *Phys. Rev. Lett.* **74**, 4388 (1995); *Phys. Lett. B* **353**, 301 (1995); *Phys. Rev. D* **53**, 2480 (1996).
- [70] M. Beneke, G. Buchalla, M. Neubert, and C. T. Sachrajda, *Phys. Rev. Lett.* **83**, 1914 (1999).
- [71] M. Beneke and M. Neubert, *Nucl. Phys.* **B675**, 333 (2003).
- [72] C.W. Bauer, D. Pirjol, I.Z. Rothstein, and I.W. Stewart, *Phys. Rev. D* **70**, 054015 (2004).
- [73] M. Beneke, G. Buchalla, M. Neubert, and C. T. Sachrajda, *Phys. Rev. D* **72**, 098501 (2005).